Local Phonon Environment as a Design Element for Long-lived Excitonic Coherence: Dithia-anthracenophane Revisited[†]

Govind Lal Sidhardh,[*,‡] Adithi Ajith,[‡] Ebin Sebastian,[¶] Mahesh Hariharan,[¶] and Anil Shaji[‡]

‡*School of Physics, Indian Institute of Science Education and Research Thiruvananthapuram, Vithura, Thiruvananthapuram, Kerala, India 695551*

¶*School of Chemistry, Indian Institute of Science Education and Research Thiruvananthapuram, Vithura, Thiruvananthapuram, Kerala, India 695551*

E-mail: govindlalsidhardh17@iisertvm.ac.in

[†]A footnote for the title

Abstract

Excitonic energy transfer in light harvesting complexes, the primary process of photosynthesis, operates with near-unity efficiency. Experimental and theoretical studies suggest that quantum mechanical wave-like motion of excitons in the pigment-protein complex may be responsible for this quantum efficiency. Observed coherent exciton dynamics can be modelled completely only if we consider the interaction of the exciton with its complex environment. While it is known that the relative orientation of the chromophore units and reorganisation energy are important design elements, the role of a structured phonon environment is often not considered. The purpose of this study is to investigate the role of a structured immediate phonon environment in determining the exciton dynamics and the possibility of using it as an optimal design element. Through the case study of dithia-anthracenophane, a bichromophore using the Hierarchical Equations Of Motion formalism, we show that the experimentally observed coherent exciton dynamics can be reproduced only by considering the actual structure of the phonon environment. While the slow dephasing of quantum coherence in dithia-anthracenophane can be attributed to strong vibronic coupling to high-frequency modes, vibronic quenching is the source of long oscillation periods in population transfer. This study sheds light on the crucial role of the structure of the immediate phonon environment in determining the exciton dynamics. We conclude by proposing some design principles for sustaining long-lived coherence in molecular systems.

Introduction

A comprehensive understanding of excited-state processes taking place in photosynthetic systems can lead to the design and development of robust energy conversion technologies. With conceptual and experimental advances in ultrafast spectroscopy, it is now possible to elucidate the dynamics behind long-range light-harvesting, excitation energy transfer and electron transfer processes at a much finer temporal resolution than ever before.[1–3] Re-

cent breakthrough experiments using 2D electronic spectroscopy[4–6] revealed the presence of long-lived coherent beatings in many light-harvesting complexes,[7,8] indicating that electronic excitations are delocalised across multiple chromophores and exist as a quantum superposition of local basis states. Quantum superpositions of local excitations are hypothesised to be the source of near-unity efficiency in photosynthetic energy transfer.[9] It should be noted, however, that that the role of quantum coherence in photosynthesis is still heavily debated. A significant number of experimental and theoretical investigations into the role of coherence have reported results that suggest otherwise.[10–12] Moreover, the proposed quantum effects are often rapidly destroyed by environment-induced fluctuations induced by the reorganisation process of the environment in a process called decoherence. Achieving control over various decoherence pathways is important for developing molecular systems with long coherence lifetimes wherein the role of quantum coherence, if any, in achieving high energy transfer efficiencies can be probed. These considerations have prompted a huge amount of theoretical and experimental research for comprehending the role of different parameters, like excitonic coupling and environment interaction, in tailoring the coherent dynamics and how their subtle balance brings about functionality.[9,13–17]

When an exciton interacts weakly with its dissipative environment, the energy transfer remains coherent for long periods of time. On the other hand, when this interaction is strong, coherence is easily lost and energy transfer can only proceed through classical hopping. As it turns out, photosynthetic chromophores belong to the intermediate coupling regime, characterised by comparable levels of interexcitonic and exciton-environment interaction. The dynamics of the exciton coupled to its environment must be studied using the methods of the theory of open quantum systems. Both weak-coupling and strong-coupling regimes of the open system (exciton in our case) allows, in many cases, for the use of powerful approximations like the Born-Oppenheimer and Markov approximation that can simplify the theoretical modelling of such systems considerably. However, the intermediate coupling regime is typically much more nuanced and consequently difficult to model mathematically.

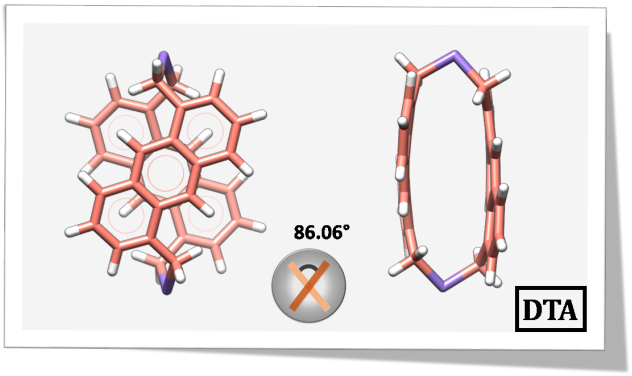

Figure 1: Ground state optimized structure of Dithia-anthracenophane. (left) top view. (right) side view. The structure was optimized using Gaussian 16 package with B3LYP functional and 6-31+G(d,p) basis.

The Hierarchical Equations Of Motion (HEOM) formalism[17,18] was developed as an appropriate tool for studying exciton dynamics in this intermediate coupling regime. HEOM unifies coherent and incoherent dynamics into a single framework and provides non-perturbative solutions. Unlike the conventional approaches like the Redfield theory,[19,20] HEOM captures the time-dependent reorganisation process of the environment and therefore is an adequate tool to study the effects of environmental phonons on excitonic energy transfer.[17]

It is known that excitonic coupling is an easily tunable parameter that can be used to control the delocalisation of electronic excitations across multiple chromophores.[21,22] Although environment interaction is also crucial in determining the exciton dynamics, the possibility of using it as a design element has not been extensively discussed previously. Most of the earlier studies ignored the detailed structure of the phonon environment and gave simple phenomenological descriptions to it.[13,16–18] The importance of considering the bath structure became evident when several studies showed that the presence of strongly coupled quasi-resonant nuclear modes could significantly boost the energy transfer efficiency in heterodimers.[16,23,24] Yet, a detailed understanding of this aspect is lacking.

A number of recent theoretical and experimental studies have been conducted on simple dimer systems, shedding light into the role of different factors in engineering long-lived coherence.[23–25] In addition to these, coherent oscillation of excitation energy has been re-

ported in simpler synthetic systems with small excitonic coupling and large reorganisation energy; a regime where long-lived coherence is not expected since large reorganisation energy is typically associated with strong fluctuations in electronic energy gap which tends to quickly destroy coherence.[26,27] In the current study, we consider the case of one such near orthogonal bi-chromophore system, dithia-anthracenophane (DTA), for which experimental evidence suggests long-lived quantum coherence with a dephasing time of 1.0 ±0.1 ps and oscillation period of 1.2 ±0.2 ps.[26,28–30] We seek the origin of this long-lived coherence despite the large reorganisation energy. This article is organised as follows: Section 2 provides a brief description of the theory and methods used. In section 3, the main results are presented, and the main implications discussed. Finally, the concluding remarks are presented in section 4.

Methods

Dithia-anthracenophane is a bi-chromophoric system consisting of two anthracene units arranged almost perpendicular to each other and linked together by two methylene-sulphur-methylene bridges. The ground state optimised structure of DTA is shown in Fig. 1. X-ray structure analysis shows that the planes of the two anthracene units are parallel to each other, separated by a distance of 3.41 Å. The rotational angle between the longer axis of the two anthracene units is about 86.06°.[28] A detailed theoretical study on the electronic properties of DTA has been published elsewhere.[30]

Exciton dynamics in DTA can be studied as the dynamics of localised Frenkel excitons[31] in the two anthracene units. The localised excitons span an effective two-state space interacting via the excitonic coupling. Upon excitation, the dimer system will be in a coherent superposition of these two states. The system then loses this coherence by interacting with an environment consisting of intramolecular (nuclear) degrees of freedom and solvent degrees of freedom. We assume that the localised excitons only interact with the phonons in its immediate vicinity (immediate phonon environment). This uncorrelated-bath approxi-

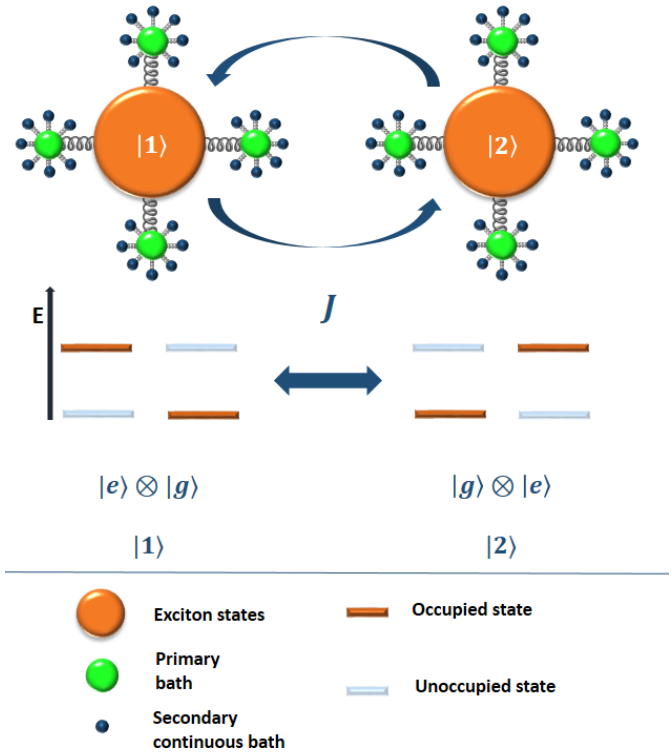

Figure 2: An illustration of the system-bath interaction model assumed in this study. The system directly interacts with the primary bath which is in turn coupled to the dissipative secondary bath.

mation is backed by several recent studies that did not find any such correlations between local baths.[32–34] According to the detailed theory of decoherence,[35] coupling between the localized excitons and mutually uncorrelated local baths will have the effect of localizing any excitons that may lie delocalized across multiple chromophores. In other words, the initial excitation, which is a coherent superposition of two delocalized states, tends to be localized again by the bath through the removal of this coherence. The nuclear degrees of freedom are modelled as a discrete primary harmonic bath, which is in turn coupled to a secondary continuous thermal bath consisting of solvent degrees of freedom and any other residual degrees.[36] It is also assumed that the excitons are not directly coupled to the secondary bath. This assumption is valid if the exciton-solvent interaction is weak; In the case of the molecule considered in this work, intramolecular modes account for most of the total reorganisation energy, meaning that the solvent contribution is rather small. Since reorganisation energy is

directly related to coupling strength, this indicates that the exciton-solvent interaction may be assumed to be weak. In our model, only the exciton forms part of the system, and all the vibrational modes are assumed to be part of the environment. An alternate approach, which is particularly useful when studying the dynamics of the vibronic states itself, is to consider the exciton and primary modes as part of the system.[16,37] However, since we are only interested in the dynamics of the exciton in this work, we chose the former model. The system-environment interaction is described by a spectral density representing the coupling strength of each bath mode to the system. Fig. 2 is an illustration of the system-bath interaction model discussed above.

The total Hamiltonian, $\mathcal{H}$ takes the form of the Frenkel exciton Hamiltonian[17,36] given by

$$\mathcal{H} = \mathcal{H}_{sys} + \mathcal{H}_{bath} + \mathcal{H}_{sb} + \mathcal{H}_{reorg} \tag{1}$$

$\mathcal{H}_{sys}$ is the system Hamiltonian, defined as

$$\mathcal{H}_{sys} = \epsilon_1 |1\rangle \langle 1| + \epsilon_2 |2\rangle \langle 2| + J(|1\rangle \langle 2| + |2\rangle \langle 1|) \tag{2}$$

ϵ_i is the excitation energy associated with the i^{th} site. J is the excitonic coupling between the two sites. $|i\rangle$ represents the state with only the i^{th} site excited.

$\mathcal{H}_{bath}$ is the bath Hamiltonian, and it represents the energy of the primary and secondary harmonic baths. $\mathcal{H}_{reorg}$ is the renormalisation term in the spin-boson model arising due to reorganisation process. Physically this term corresponds to the energy dissipated when the molecule equilibrates from the Frank-Condon geometry to the excited state-geometry. $\mathcal{H}_{sb}$ is the interaction Hamiltonian representing the system-bath interaction. This interaction is assumed to be linear and, because of the system-bath interaction model chosen, $\mathcal{H}_{sb}$ separates into two terms representing the system-primary bath interaction and primary bath-secondary bath interaction. The system-primary bath coupling strength is determined

by the displacement of the primary bath modes from Frank-Condon geometry upon equilibration and, therefore, may be explicitly calculated given the ground state and excited state geometries. The exact form of the terms in Eq.1 is given in the supporting information.

In the reduced system density operator approach to dissipative quantum dynamics, the object of interest is the Reduced Density Operator (RDO) of the exciton, $\rho(t)$, which is the partial trace of the total density operator $\rho_{total}(t)$ over the bath degrees of freedom. The bath effects enter into the RDO through the bath correlation function,[18] which is related to the bath spectral density[38] via the fluctuation-dissipation theorem.[38,39] Fluctuation-dissipation theorem directly relates fluctuations in electronic energy gap to reorganisation energy dissipation. The correlation function quantifies fluctuations and the spectral density describes energy dissipation per bath mode. We assume that initially, only one of the sites is excited and that the two-level system is uncorrelated to the bath.

Several forms of the bath spectral density are employed in the literature; the ohmic spectral densities, which assumes a linear relation to the bath frequencies, being the most widely used among them. However, these are just phenomenological descriptions often adopted for computational simplicity. While these simple descriptions do give useful physical insights, they cannot represent the well-structured exciton-bath interactions found in real molecules. This rich structure arises from strong coupling of the excitons to intramolecular vibrations, and representing these requires a highly expressive spectral density model. For the system-bath interaction model considered in this work, an appropriate form of the spectral density is the Multimode Brownian Oscillator[27] (MBO) model. For the ξ^{th} primary vibrational mode of site j, the MBO spectral density is given by[36,38]

$$\mathcal{J}_{j\xi}(\omega) = 2S_{j\xi}\omega_{j\xi}\frac{\omega\omega_{j\xi}^2\varphi_{j\xi}(\omega)}{(\omega^2-\omega_{j\xi}^2)^2+\varphi_{j\xi}^2(\omega)\omega^2} \tag{3}$$

Here, $S_{j\xi}$,$\omega_{j\xi}$ are respectively the Huang-Rhys factor and natural frequency of the primary bath mode considered. These factors are in turn related to the reorganisation energy of

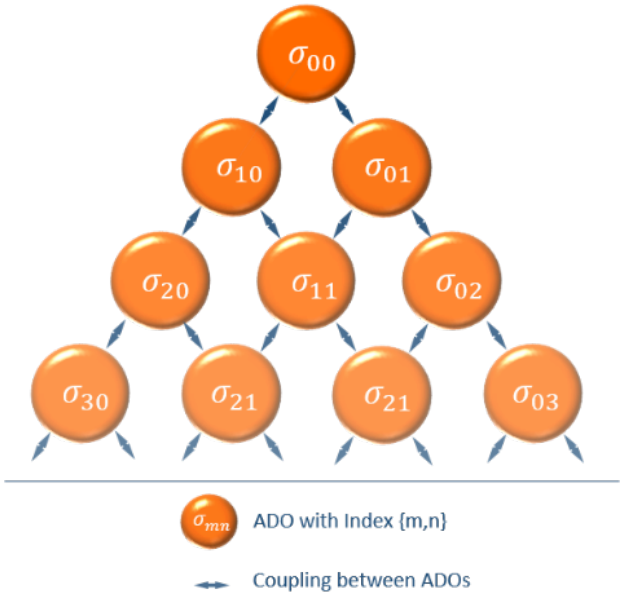

Figure 3: An illustration of the Hierarchical Equations Of Motion formalism for the simple case of a two-level system interacting with Drude-Debye bath at high temperature.8 Each node in the tree represents an ADO indexed by two numbers. The two-sided coupling between the ADOs is shown by the double-headed blue arrows. σ_{00} is the reduced system operator, and all the remaining ADOs encode the system-bath interaction. Each level of the tree is called a hierarchy. In this case, the HEOM is terminated at the third hierarchy.

the mode as $\lambda_{j\xi} = S_{j\xi}\omega_{j\xi}$. The total spectral density associated with site is, therefore, $\mathcal{J}_j = \sum_\xi \mathcal{J}_{j\xi}$. The factor $\varphi_{j\xi}(\omega)$ characterises the primary bath-secondary bath interaction and is referred to as the 'friction' term. It is analogous to friction in the sense that higher values of the parameter correspond to quicker relaxation of the nuclear mode and vice versa. Thus, when $\omega_{j\xi} > \varphi_{j\xi}(\omega)$, Eq.3 represents an underdamped nuclear mode. Indeed the MBO model reduces to the often used Drude-Debye model[38] in the overdamped regime ($\varphi_{j\xi} \gg \omega_{j\xi}$). If through spectroscopic means or other methods, one can find intramolecular vibrational modes that are strongly coupled to the exciton, Eq.(3) can be used to give a more realistic description of the phonon environment to the exciton which includes the effects of the interaction between the primary and secondary bath modes as well.

The Hierarchical Equations Of Motion (HEOM) formalism was used to propagate the reduced density operator. The HEOM formalism, first introduced by Tanimura and Kubo,[18] and significantly developed thereafter, captures the strong non-markovian dynamics asso-

ciated with the time-dependent reorganisation process and gives non-perturbative, exact solutions.[17] Detailed discussions about the formalism and its derivation using the path integral techniques and stochastic unravelling method can be found in the references.[17,40] In this technique, the system-bath interaction is decomposed into, what are called, Auxilliary Density Operators (ADO). Each ADO is labelled by a unique index and categorised into levels called hierarchies based on their contribution to the overall dynamics. The time evolution of the ADOs and the RDO are linked together through an infinite set of coupled differential equations called the Hierarchical Equations Of Motion. HEOM is then truncated at a finite level of hierarchy and numerically integrated to obtain the system dynamics. An illustration of HEOM is given in Fig. 3. Several forms of HEOM which, in principle, works with arbitrary spectral densities have been presented in the literature.[41–43] For the particular case when the bath correlation function can be written as a sum of exponential terms, the HEOM takes the following simpler form,[16–18,40]

$$\dot{\sigma}_n(t) = -(i\mathcal{L}_{sys} + \sum_{j,k} n_{jk}\gamma_{jk})\sigma_n(t) + \sum_{j,k} \Phi_j \sigma_{n_{jk}^+} + \sum_{j,k} \Theta_{jk}\sigma_{n_{jk}^-} \tag{4}$$

Where Θ_{jk}, γ_{jk} and Φ_j are operators that depend on the expansion terms in the correlation function and projection operators $|j\rangle\langle j|$. $\mathcal{L}_{sys}$ is the system Liouville operator. In Eq.4, σ_n is the ADO identified by the index array, n. $\sigma_{n_{jk}^{\pm}}$ represents the ADO with the n_{jk}^{th} component of index array replaced by $(n_{jk} \pm 1)$. By construction, the zeroth tier ADO, $\sigma_{\vec{0}}(t) := \rho(t)$, is the reduced system density operator. With the MBO model for the system-bath interaction, bath correlation functions can be expanded as a sum of exponentials,[36,38] thus facilitating the use of Eq.4 to solve the exciton dynamics.

The HEOM method is notorious for its computational complexity. Calculations quickly become computationally intractable as the bath structure becomes more complex. Therefore, an efficient implementation of HEOM posed one of the most demanding tasks in this study. Our implementation of HEOM is parallelisable and designed for optimal run-time. The software package written by us is implemented in Intel Fortran 19.0 and parallelly executed

on twenty eight Intel(R) Xeon(R) Gold 6132 processors for all the computations done in this work. The exact form of the functions, the algorithms used and other details regarding the implementation of HEOM is provided in the supporting information.

The excitonic coupling between the chromophores can be approximated to the coulombic interaction between the generalised transition charge densities.[44,45] This approximation is valid if the transition densities do not overlap significantly.[44] The Transition Density Cube Method (TDCM) developed by Krueger et al. can then be used to calculate this coulombic interaction between the Frenkel excitons.[45] The method is exact within the Frenkel exciton model and works by coarse-graining space into discrete cubical elements and replacing the volume integral in Coulomb's law with a sum over these discretised elements. The transition density of the monomeric part of DTA can be approximated to that of 1,5-dimethylanthracene and was estimated using TD-DFT[46]/CAM-B3LYP[47] functional with 6-31G(d,p) basis set. The basis set for this calculation and later calculations were chosen to be similar to the ones used in Ref.30, and convergence was ensured using the inbuilt accuracy controls in the Gaussian package. We also made sure the results were consistent with the results in Ref.30. The transition density distribution was extracted using the Multiwfn package[48] from Gaussian 16[49] output file.

Results and discussion

The excitonic coupling in DTA was estimated to be 43.3 cm^{-1}. The calculations were done in vacuum and therefore, must be corrected for solvent effects. There are two effects due to the solvent on the excitonic coupling, screening- which tends to reduce the effective excitonic coupling and polarisation- which tends to increase it.[30] For DTA in Tetrahydrofuran (THF), it was shown that the polarisation effect tends to nullify the screening effect and the effective excitonic coupling is slightly higher than the vacuum value. In a more detailed analysis given in Ref.30 excitonic coupling in DTA in THF was estimated to lie in the range 50-100 cm^{-1}.

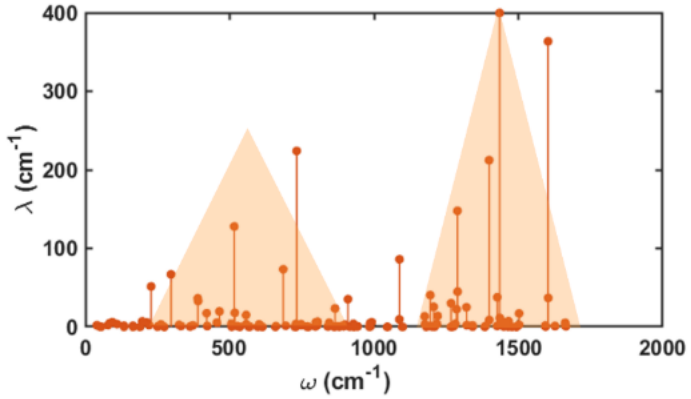

(a)

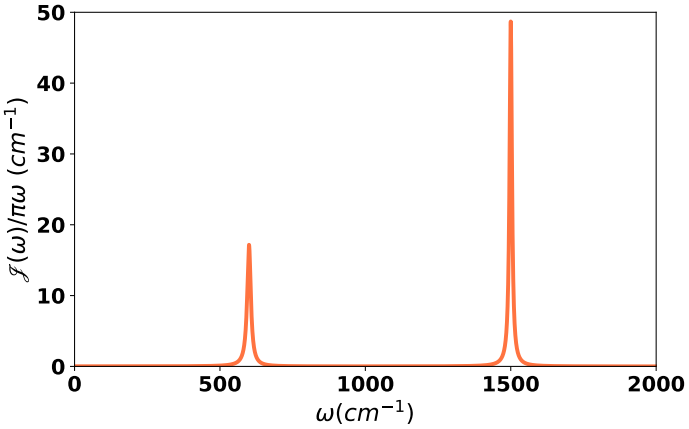

(b)

Figure 4: (a)Distribution of reorganisation energy (λ) among nuclear modes in DTA. Two major clusters (represented by triangles) of nuclear modes located around 600 cm^{-1} and 1500 cm^{-1} can be seen. A simplified environment is constructed by replacing each of these clusters with effective nuclear modes. (b) Distribution of reorganisation energy with the employed MBO model Eq. (3) is shown. This simplified bath includes two nuclear modes of frequencies 600 cm^{-1} and 1500 cm^{-1} respectively, with Huang-Rhys factors 0.674 and 0.51 and decay terms 15 cm^{-1} and 10 cm^{-1} respectively.

This straightaway leads to a discrepancy between the calculated value and the experimental estimate[50] of 17.5 cm^{-1} in THF. We shall address this issue later on.

To obtain an estimate of the coupling strength of each nuclear mode to the exciton, we conducted an excited state vibronic analysis on DTA using the Gaussian 16 package. The structure of the S1 state of DTA was optimised using CIS theory[51] and 6-31+G(d,p) basis set. A plot showing the distribution of the reorganisation energy of each nuclear mode of DTA is shown in Fig. 4a. The total reorganisation energy of the monomeric part can then

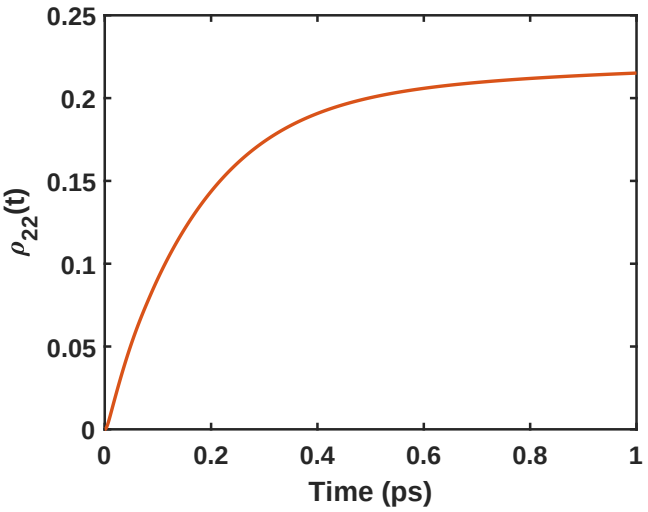

Figure 5: Time evolution of the exciton population in the site basis. Excitonic coupling was set to 55 cm^{-1} and the system-bath interaction is modelled as the Drude-debye density with reorganization energy λ=1634.8 cm^{-1} and cutoff frequency γ=10 cm^{-1}. No signature of quantum coherence is observed and also population transfer is very slow, in contradiction with the experimental observation.

be estimated as 1634.8 cm^{-1}.

We first calculated the exciton dynamics in DTA with the parameters calculated above and the often-used, unstructured Drude-Debye[38] spectral density with a cut-off frequency of 10 cm^{-1}. All calculations in this work were done with the temperature set to 300K. The calculated dynamics, however, does not show any signs of coherence and has meagre energy transfer rates (Fig. 5). Thus we see that an unstructured system-bath model does not predict the experimentally observed long-lived coherence in DTA.

The distribution in Fig. 4a has a complex structure with clusters of strongly coupled nuclear modes around 600 cm^{-1} and 1500 cm^{-1}. There are also a few weakly coupled ($S \sim 0.01$) nuclear modes involving the vibrations of the C-H bonds with frequencies around 3000 cm^{-1}. Because of their low coupling strength and high frequency, they do not affect the exciton dynamics significantly and are, therefore, ignored in the analysis. It should also be noted that there is a negligible contribution to the total reorganisation energy from the low-frequency end of the spectrum. Comparing this distribution with the reorganisation energy density ($\mathcal{J}(\omega)/\pi\omega$) of the Drude-Debye model, one immediately sees that the Drude-

Debye model poorly describes the actual structure of the local phonon environment. In fact, the most strongly coupled nuclear modes in the Drude-Debye model lie in the low-frequency region in strict contradiction to the actual structure of the primary bath. The inability of the Drude-Debye model to predict the observed dynamics shows the importance of the structure of the local phonon environment in determining the exciton dynamics.

Because of the symmetry of the molecule, we approximate the primary bath of the Frenkel excitons to have the same structure as in Fig. 4a but only half the reorganisation energy per mode. To reduce the computational complexity involved in solving the HEOM, we make the following simplifications. Each of the two groups of strongly coupled nuclear modes (shown in Fig. 4a) is replaced with an effective mode, centred at 600 cm^{-1} and 1500 cm^{-1} , respectively, such that these effective modes dissipate the same amount of reorganisation energy as its parent group. The Huang-Rhys factors of these effective modes are, therefore, 0.674 and 0.51, respectively. We now model this bath using the MBO model with the above mentioned nuclear modes and appropriate decay parameters. Fig. 4b shows the reorganisation energy density for the corresponding bath, with decay parameters set to 15 cm^{-1} and 10 cm^{-1} respectively for the 600 cm^{-1} mode and the 1500 cm^{-1} mode. As we will show, even with this simplified description of the phonon bath, we were able to reproduce the observed excitation dynamics. This simple construction also gives valuable physical insights into the mechanism through which long-lived excitonic coherence is maintained in the molecule.

With the primary bath consisting of the above mentioned two effective modes and the excitonic coupling set in the range 50-100 cm^{-1}, we solve for the exciton dynamics for several values of friction terms using HEOM. The friction term is treated as an empirically determined parameter. With the excitonic coupling set to 55 cm^{-1} and the friction term of the effective nuclear modes set to 15 cm^{-1} and 10 cm^{-1}, respectively, the simulated dynamics agree very well the experimental observation. Fig. 6a shows the resultant dynamics, with the abscissa representing the exciton population in the site basis and time along the ordinate. Fig. 6b shows the corresponding plots of the off-diagonal terms of the density matrix in the

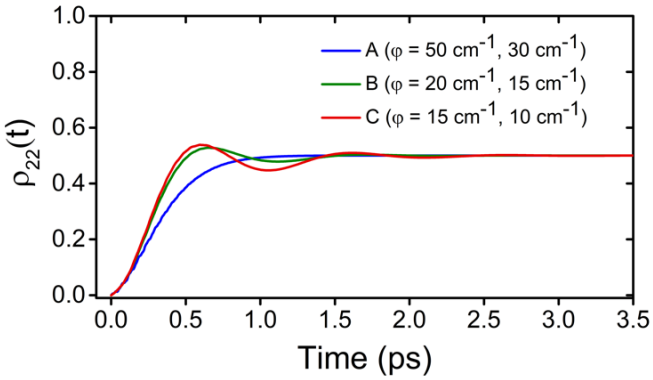

(a)

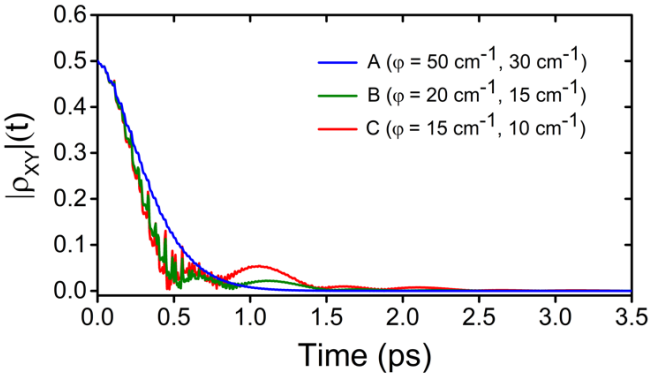

(b)

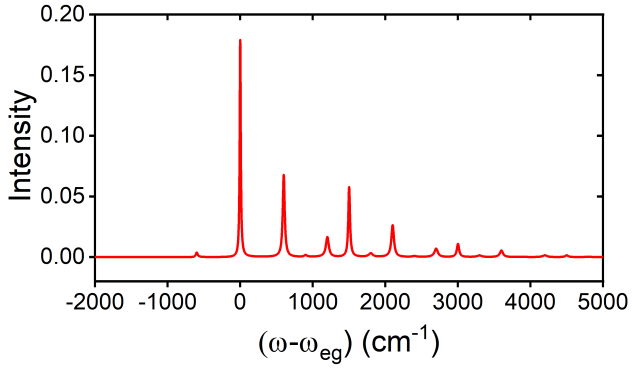

(c)

Figure 6: (a) Exciton population dynamics of the second site plotted against time. (b) Time evolution of the absolute value of off-diagonal term of density matrix in exciton basis. The excitonic coupling strength of the homodimer is set to 55 cm^{-1}. The primary bath consists of two effective modes with Huang-Rhys factors 0.674 and 0.51 and frequencies 600 cm^{-1} and 1500 cm^{-1} respectively. Coherence life time increases as the friction term (f) is decreased. With the friction terms set to 15 cm^{-1} and 10 cm^{-1}, the resultant dynamics agree well with the experimental observation. (c) The unnormalised absorption spectra of the model employed, when the friction terms are set to 15 cm^{-1} and 10 cm^{-1}. ω_{eg} is the excitation energy from the ground to the excited state.

exciton basis. A progressive change from incoherent to coherent dynamics is seen as the friction term is decreased. We see that with a more realistic description of the immediate phonon environment, the HEOM formalism predicts the experimentally observed coherent dynamics. More specifically, the leading oscillating term in curve C of Fig.6a has a time period of 1ps, in agreement with the experimental estimate of 1.2 ± 0.2ps.[26] By fitting the local maxima of the curve to an exponential term, we estimate the dephasing time of the curve to be around 0.82ps, also in agreement with the experimental estimate of 1 ± 0.1 ps. Fig.6c shows the absorption spectrum of the employed model, for decay terms 15 cm^{-1} and 10 cm^{-1}, for the 600 cm^{-1} and 1500 cm^{-1} modes, respectively. The absorption spectrum contains narrow peaks as expected from the environment model chosen. The spectrum is, however, more sharply peaked than the experimentally obtained spectra in Ref.26. Among other reasons, the simplified two-mode form of the bath could be a contributing factor to this difference. In addition, the relatively large Huang-Rhys factor of the effective modes, in comparison to the actual vibrational modes of the molecule itself and to other light-harvesting complexes in general, is also a consequence of the simplification employed. This could be the reason behind the relatively low decay terms in curve C of Fig.6a as well. Moreover, adding more nuclear modes to the primary bath makes the problem computationally intractable.

Now we attempt to give a physical explanation as to how coherence is sustained in DTA despite its relatively high reorganisation energy and small excitonic coupling. Notice that a large portion of the reorganisation energy is being dissipated by the high-frequency modes around 600 cm^{-1} and 1500 cm^{-1}. Such high-frequency modes are typically underdamped and dissipate the reorganisation energy slowly.[38] This slow rate of dissipation induces only small fluctuations in the energy levels of the system and hence results in a slow rate of decoherence.

There is another aspect that needs to be pointed out. It was mentioned earlier that the bare excitonic coupling calculated using TDCM and other *ab initio* methods is much larger than the experimental estimate of 17.5 cm^{-1}. There is extensive literature on why *ab initio*

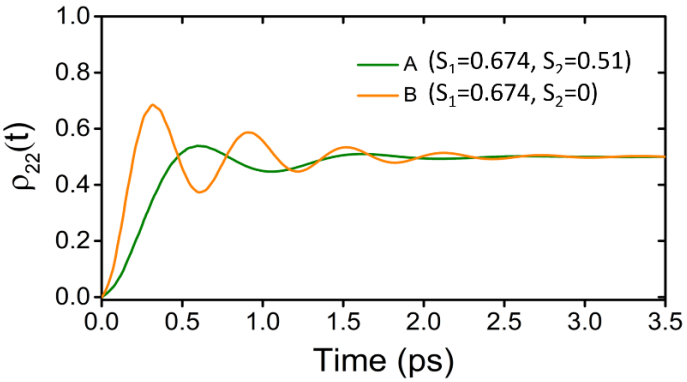

Figure 7: The time evolution of exciton population is two scenarios. (A-Green curve) The exciton is coupled to the effective modes with Huang Rhys factors: 0.674 and 0.51. The Friction term for both modes are set to 15 cm^{-1} and 10 cm^{-1} respectively. (B-Yellow curve) The exciton is only coupled to the effective nuclear mode at 600 cm^{-1} with Huang Rhys factor: 0.51. The friction term is set to 15 cm^{-1}. The reduction in frequency of the green curve is due to vibronic quenching.

calculations of excitonic splitting give overestimated values, and it is often attributed to an effect called vibronic quenching.[52–54] It refers to the quenching or reduction of excitonic splitting due to the coupling between excitonic states and vibrational states. This can be thought of as due to the localising tendency of vibrational modes on the excitons. A simple perturbative analysis shows that the quenching factor can be estimated as $\Gamma = \exp(-\sum S_i)$.[52–54] We now show that this is what is happening in DTA. The exciton dynamics was recalculated with all parameters kept the same, except that the Huang-Rhys factor of the effective mode at 1500 cm^{-1} was set to zero. This is simply assuming that the exciton is not coupled to this nuclear mode. As can be seen from Fig. 7, the time period of the resultant dynamics has decreased by a factor of about 2, consistent with the quenching factor of the removed mode: $\exp(-0.51) \approx 0.6$. This indicates that vibronic quenching is the source of the discrepancy between the calculations and experimental estimation of excitonic coupling.

There is extensive evidence that quasi-resonant modes can significantly boost coherence lifetimes and energy transfer efficiency in heterodimers.[9,16] It is therefore worth looking if such an advantage can be expected in homodimers like DTA. To see this, we calculated the exciton dynamics in the hypothetical setting of a homodimer with an excitonic coupling of

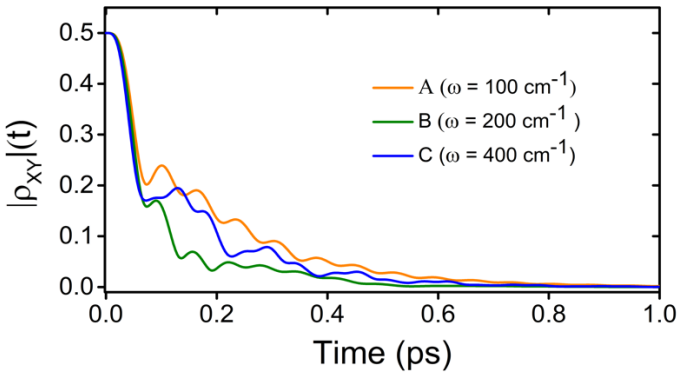

Figure 8: Time evolution of the off-diagonal elements of the density matrix in the exciton basis. A hypothetical homodimer with an excitonic coupling of 100 cm^{-1} is considered as the system. Each site is coupled to a low energy thermal bath represented by a Drude-debye model with reorganisation energy of 20 cm^{-1} and cut-off frequency 53.08 cm^{-1}. Each site is also strongly coupled (S=0.1) to a nuclear mode, the frequency of which is varied but the friction term is fixed at 50 cm^{-1}. It can be seen that the coherence lifetime is reduced as the frequency approaches the resonant condition of 200 cm^{-1}.

100 cm^{-1}; the primary bath coupled to the exciton consists of a low energy thermal bath and a single nuclear mode. It can be seen from Fig. 8 that as the nuclear mode becomes resonant (ω=200 cm^{-1}) with the excitonic splitting, the decoherence rate increases. This shows that the presence of quasi-resonant modes tends to reduce the coherence lifetime in homodimers. It is not difficult to see why this is the case. Detuning of energy levels tends to reduce population transfer. In heterodimers, sites are highly detuned, and therefore, in the absence of resonant modes, population transfer is rather small; but coupling to resonant modes creates ladders of vibronic states with almost no detuning, thus facilitating maximum population transfer. In homodimers, sites are of almost equal energy; hence, coherent population transfer is maximum, even in the absence of resonant modes. In other words, the coupling to resonant modes does not bring about any advantage in population transfer. On the contrary, it opens up new dissipation pathways, which adds to decoherence (as seen in Fig. 8). This comparison shows that coupling to intramolecular modes is a double-edged sword; a subtle balance between the decoherence induced by the intramolecular modes and the enhanced population transfer induced by vibronic states is required to bring about functionality.

Conclusion

Now, we return to our original question. Is the structure of the immediate phonon environment significant in determining the exciton dynamics? If so, can we engineer the local environment to establish control over it? We tried to find answers to these questions by looking at the specific case of DTA for which experimental evidence of long-lived coherence is available.

We showed that with other factors like the excitonic coupling and reorganisation energy remaining the same, an unstructured environment like the Drude-Debye model do not predict the long-lived coherence observed in DTA. Indeed, the vibronic analysis conducted on the molecule showed that the immediate phonon environment has a non-trivial structure with a significant portion of reorganisation energy being dissipated by high-frequency nuclear modes. With the MBO model, we constructed a simplified two-mode representation of this primary bath, and the simulated dynamics showed long-lived coherence with the time period and coherence lifetime, agreeing well with the experimental observation. We also showed that vibronic coupling tends to reduce the bare excitonic coupling due to what is called vibronic quenching; this is the cause of the discrepancy between the experimental and calculated values of excitonic splitting. These observations show that the immediate phonon environment plays a crucial role in determining the exciton dynamics.

The question as to what extent one can control the coherent exciton dynamics by designing the environment is, however, not a simple question one to answer. It requires a more detailed and thorough analysis of the effects of the local phonon environment, covering a much larger parameter space than what was considered in this study. It also depends on a lot of practical considerations; for example, manipulating the structure of the molecule may affect the electronic properties and other desirable features of the molecule. However, the results of this study do give some valuable insights in this direction.

Since one is often interested in protecting coherence for longer time periods, we focus on this direction. It is well known that building molecules that are rigid, therefore having lower

reorganisation energy, is one way of sustaining long term coherence. However, this is not always practically possible. From our current study, we propose that one could place a far more realistic constraint that is instead of looking for rigid molecules, one can build 'adiabatic' ones. By 'adiabatic' we refer to molecules that undergo slow reorganisation process. This can be achieved by designing systems such that the strongly coupled nuclear modes are in the high-frequency domain, and by minimising the exciton-solvent interaction. We also observed that for homodimers, coupling to quasi-resonant modes results in a reduction of the coherence lifetime and hence should be avoided while designing the molecule. Vibronic quenching forms an additional constraint that also needs to be accounted for. These form some of the directions one can move in while designing chromophoric systems to achieve long term excitonic coherence.

A complete understanding of how the immediate phonon environment affects the exciton dynamics and to what extent one can design this environment to achieve control over coherent exciton dynamics requires much more in-depth analysis and understanding of practical constraints. Our work provides the first steps in this direction. In future works, we explore the practical constraints involved and understand how they limit our proposals.

Acknowledgement

A. S. acknowledges the support of the Science and Engineering Research Board of the Department of Science and Technology, Government of India through grant no. EMR/2016/007221, the QuEST program of the Department of Science and Technology through project No. Q113 under Theme 4. M.H acknowledges the support of the Science and Engineering Research Board, Department of Science and Technology, Government of India through grant no. CRG/2019/002119; the Nanomission project (DST/NM/TUE/EE01/2019) of the Department of Science and Technology, Government of India. G.L.S is thankful for the DST-INSPIRE Fellowship. E.S acknowledges UGC for the research fellowship. The authors

acknowledge the use of the *Padmanabha* computational cluster made available through the center for High Performance Computation at IISER TVM.

Supporting Information Available

The exact form of the HEOM with the MBO model, the details regarding the implementation of HEOM and convergence details are given in the supporting information.

References

(1) Rosker, M.; Wise, F.; Tang, C. Femtosecond relaxation dynamics of large molecules. *Physical review letters* **1986**, *57*, 321.

(2) Nelson, K. A.; Williams, L. R. Femtosecond time-resolved observation of coherent molecular vibrational motion. *Physical review letters* **1987**, *58*, 745.

(3) Zewail, A. H. Laser femtochemistry. *Science* **1988**, *242*, 1645–1653.

(4) Jonas, D. M. Two-dimensional femtosecond spectroscopy. *Annual review of physical chemistry* **2003**, *54*, 425–463.

(5) Brixner, T.; Stenger, J.; Vaswani, H. M.; Cho, M.; Blankenship, R. E.; Fleming, G. R. Two-dimensional spectroscopy of electronic couplings in photosynthesis. *Nature* **2005**, *434*, 625–628.

(6) Cho, M.; Vaswani, H. M.; Brixner, T.; Stenger, J.; Fleming, G. R. Exciton Analysis in 2D Electronic Spectroscopy. *The Journal of Physical Chemistry B* **2005**, *109*, 10542–10556, PMID: 16852278.

(7) Engel, G. S.; Calhoun, T. R.; Read, E. L.; Ahn, T.-K.; Mančal, T.; Cheng, Y.-C.; Blankenship, R. E.; Fleming, G. R. Evidence for wavelike energy transfer through quantum coherence in photosynthetic systems. *Nature* **2007**, *446*, 782–786.

(8) Lee, H.; Cheng, Y.-C.; Fleming, G. R. Coherence dynamics in photosynthesis: protein protection of excitonic coherence. *Science* **2007**, *316*, 1462–1465.

(9) Scholes, G. D.; Fleming, G. R.; Chen, L. X.; Aspuru-Guzik, A.; Buchleitner, A.; Coker, D. F.; Engel, G. S.; Van Grondelle, R.; Ishizaki, A.; Jonas, D. M. et al. Using coherence to enhance function in chemical and biophysical systems. *Nature* **2017**, *543*, 647–656.

(10) Tempelaar, R.; Jansen, T. L.; Knoester, J. Vibrational beatings conceal evidence of electronic coherence in the FMO light-harvesting complex. *The Journal of Physical Chemistry B* **2014**, *118*, 12865–12872.

(11) Duan, H.-G.; Prokhorenko, V. I.; Cogdell, R. J.; Ashraf, K.; Stevens, A. L.; Thorwart, M.; Miller, R. D. Nature does not rely on long-lived electronic quantum coherence for photosynthetic energy transfer. *Proceedings of the National Academy of Sciences* **2017**, *114*, 8493–8498.

(12) Cao, J.; Cogdell, R. J.; Coker, D. F.; Duan, H.-G.; Hauer, J.; Kleinekathofer, U.; Jansen, T. L.; Mančal, T.; Miller, R. D.; Ogilvie, J. P. et al. Quantum biology revisited. *Science advances* **2020**, *6*, eaaz4888.

(13) Ishizaki, A.; Fleming, G. R. Theoretical examination of quantum coherence in a photosynthetic system at physiological temperature. *Proceedings of the National Academy of Sciences* **2009**, *106*, 17255–17260.

(14) Romero, E.; Augulis, R.; Novoderezhkin, V. I.; Ferretti, M.; Thieme, J.; Zigmantas, D.; Van Grondelle, R. Quantum coherence in photosynthesis for efficient solar-energy conversion. *Nature physics* **2014**, *10*, 676–682.

(15) Fleming, G. R.; Schlau-Cohen, G. S.; Amarnath, K.; Zaks, J. Design principles of photosynthetic light-harvesting. *Faraday discussions* **2012**, *155*, 27–41.

(16) O'Reilly, E. J.; Olaya-Castro, A. Non-classicality of the molecular vibrations assisting exciton energy transfer at room temperature. *Nature communications* **2014**, *5*, 1–10.

(17) Ishizaki, A.; Fleming, G. R. Unified treatment of quantum coherent and incoherent hopping dynamics in electronic energy transfer: Reduced hierarchy equation approach. *The Journal of chemical physics* **2009**, *130*, 234111.

(18) Tanimura, Y.; Kubo, R. Time evolution of a quantum system in contact with a nearly Gaussian-Markoffian noise bath. *Journal of the Physical Society of Japan* **1989**, *58*, 101–114.

(19) Redfield, A. G. On the theory of relaxation processes. *IBM Journal of Research and Development* **1957**, *1*, 19–31.

(20) Redfield, A. *Advances in Magnetic and Optical Resonance*; Elsevier, 1965; Vol. 1; pp 1–32.

(21) Yamagata, H.; Maxwell, D.; Fan, J.; Kittilstved, K.; Briseno, A.; Barnes, M.; Spano, F. HJ-aggregate behavior of crystalline 7, 8, 15, 16-tetraazaterrylene: introducing a new design paradigm for organic materials. *The Journal of Physical Chemistry C* **2014**, *118*, 28842–28854.

(22) Hestand, N. J.; Spano, F. C. Molecular aggregate photophysics beyond the Kasha model: novel design principles for organic materials. *Accounts of chemical research* **2017**, *50*, 341–350.

(23) Tiwari, V.; Peters, W. K.; Jonas, D. M. Electronic resonance with anticorrelated pigment vibrations drives photosynthetic energy transfer outside the adiabatic framework. *Proceedings of the National Academy of Sciences* **2013**, *110*, 1203–1208.

(24) Halpin, A.; Johnson, P. J.; Tempelaar, R.; Murphy, R. S.; Knoester, J.; Jansen, T. L.;

Miller, R. D. Two-dimensional spectroscopy of a molecular dimer unveils the effects of vibronic coupling on exciton coherences. *Nature chemistry* **2014**, *6*, 196–201.

(25) Hayes, D.; Griffin, G. B.; Engel, G. S. Engineering coherence among excited states in synthetic heterodimer systems. *Science* **2013**, *340*, 1431–1434.

(26) Yamazaki, I.; Akimoto, S.; Yamazaki, T.; Sato, S.-i.; Sakata, Y. oscillatory excitation transfer in dithiaanthracenophane: Quantum beat in a coherent photochemical process in solution. *The Journal of Physical Chemistry A* **2002**, *106*, 2122–2128.

(27) Zhu, F.; Galli, C.; Hochstrasser, R. The real-time intramolecular electronic excitation transfer dynamics of 9', 9-bifluorene and 2', 2-binaphthyl in solution. *The Journal of chemical physics* **1993**, *98*, 1042–1057.

(28) Sakata, Y.; Toyoda, T.; Misumi, S.; Yamazaki, T.; Yamazaki, I. Synthesis of dithia (1, 5)[3.3] anthracenophane with crossed structure and its excimer emission. *Tetrahedron letters* **1992**, *33*, 5077–5080.

(29) Alfonso Hernandez, L.; Nelson, T.; Tretiak, S.; Fernandez-Alberti, S. Photoexcited energy transfer in a weakly coupled dimer. *The Journal of Physical Chemistry B* **2015**, *119*, 7242–7252.

(30) Yang, L.; Caprasecca, S.; Mennucci, B.; Jang, S. Theoretical investigation of the mechanism and dynamics of intramolecular coherent resonance energy transfer in soft molecules: A case study of dithia-anthracenophane. *Journal of the American Chemical Society* **2010**, *132*, 16911–16921.

(31) Frenkel, J. On the transformation of light into heat in solids. I. *Physical Review* **1931**, *37*, 17.

(32) Olbrich, C.; Strumpfer, J.; Schulten, K.; Kleinekatofer, U. Quest for spatially correlated

fluctuations in the FMO light-harvesting complex. *The Journal of Physical Chemistry B* **2011**, *115*, 758–764.

(33) Van Der Vegte, C.; Prajapati, J.; Kleinekatofer, U.; Knoester, J.; Jansen, T. Atomistic modeling of two-dimensional electronic spectra and excited-state dynamics for a light harvesting 2 complex. *The Journal of Physical Chemistry B* **2015**, *119*, 1302–1313.

(34) Bondarenko, A. S.; Patmanidis, I.; Alessandri, R.; Souza, P. C.; Jansen, T. L.; de Vries, A. H.; Marrink, S. J.; Knoester, J. Multiscale modeling of molecular structure and optical properties of complex supramolecular aggregates. *Chemical science* **2020**, *11*, 11514–11524.

(35) Zurek, W. H. Decoherence, einselection, and the quantum origins of the classical. *Reviews of Modern Physics* **2003**, *75*, 715–775.

(36) Schröter, M. *Dissipative Exciton Dynamics in Light-Harvesting Complexes*; Springer, 2015; pp 4–48.

(37) Di Maiolo, F.; Painelli, A. Intermolecular energy transfer in real time. *Journal of chemical theory and computation* **2018**, *14*, 5339–5349.

(38) Mukamel, S. *Principles of nonlinear optical spectroscopy*; Oxford University Press on Demand, 1999; pp 209–260.

(39) Kubo, R.; Toda, M.; Hashitsume, N. *Statistical physics II: nonequilibrium statistical mechanics*; Springer Science & Business Media, 2012; Vol. 31; pp 31–39.

(40) Ishizaki, A.; Tanimura, Y. Quantum dynamics of system strongly coupled to low-temperature colored noise bath: Reduced hierarchy equations approach. *Journal of the Physical Society of Japan* **2005**, *74*, 3131–3134.

(41) Liu, H.; Zhu, L.; Bai, S.; Shi, Q. Reduced quantum dynamics with arbitrary bath

spectral densities: Hierarchical equations of motion based on several different bath decomposition schemes. *The Journal of chemical physics* **2014**, *140*, 134106.

(42) Tang, Z.; Ouyang, X.; Gong, Z.; Wang, H.; Wu, J. Extended hierarchy equation of motion for the spin-boson model. *The Journal of chemical physics* **2015**, *143*, 224112.

(43) Rahman, H.; Kleinekathofer, U. Chebyshev hierarchical equations of motion for systems with arbitrary spectral densities and temperatures. *The Journal of chemical physics* **2019**, *150*, 244104.

(44) You, Z.-Q.; Hsu, C.-P. Theory and calculation for the electronic coupling in excitation energy transfer. *International Journal of Quantum Chemistry* **2014**, *114*, 102–115.

(45) Krueger, B. P.; Scholes, G. D.; Fleming, G. R. Calculation of couplings and energy-transfer pathways between the pigments of LH2 by the ab initio transition density cube method. *The Journal of Physical Chemistry B* **1998**, *102*, 5378–5386.

(46) Runge, E.; Gross, E. K. Density-functional theory for time-dependent systems. *Physical Review Letters* **1984**, *52*, 997.

(47) Yanai, T.; Tew, D. P.; Handy, N. C. A new hybrid exchange–correlation functional using the Coulomb-attenuating method (CAM-B3LYP). *Chemical physics letters* **2004**, *393*, 51–57.

(48) Lu, T.; Chen, F. Multiwfn: a multifunctional wavefunction analyzer. *Journal of computational chemistry* **2012**, *33*, 580–592.

(49) Frisch, M.; Trucks, G.; Schlegel, H.; Scuseria, G.; Robb, M.; Cheeseman, J.; Scalmani, G.; Barone, V.; Petersson, G.; Nakatsuji, H. et al. Gaussian16, RevisionB. 01, Gaussian, Inc., Wallingford, CT, 2016. *Google Scholar There is no corresponding record for this reference* **2020**,

(50) Sato, S.-i.; Nishimura, Y.; Sakata, Y.; Yamazaki, I. Coherent control of oscillatory excitation transfer in dithia-1, 5 [3, 3] anthracenophane by a phase-locked femtosecond pulse pair. *The Journal of Physical Chemistry A* **2003**, *107*, 10019–10025.

(51) Fulscher, M. P.; Andersson, K.; Roos, B. O. Toward an accurate molecular orbital theory for excited states: The azabenzenes. *The Journal of Physical Chemistry* **1992**, *96*, 9204–9212.

(52) Ottiger, P.; Köppel, H.; Leutwyler, S. Excitonic splittings in molecular dimers: why static ab initio calculations cannot match them. *Chemical science* **2015**, *6*, 6059–6068.

(53) Kopec, S.; Ottiger, P.; Leutwyler, S.; Köppel, H. Vibrational quenching of excitonic splittings in H-bonded molecular dimers: Adiabatic description and effective mode approximation. *The Journal of chemical physics* **2012**, *137*, 184312.

(54) Balmer, F. A.; Ottiger, P.; Leutwyler, S. Excitonic splitting, delocalization, and vibronic quenching in the benzonitrile dimer. *The Journal of Physical Chemistry A* **2014**, *118*, 11253–11261.

TOC Graphic

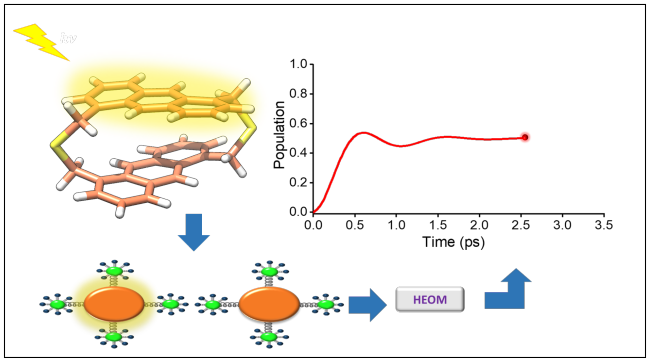
hν
Population
1.0
0.8
0.6
0.4
0.2
0.0
0.0
0.5
1.0
1.5
2.0
2.5
3.0
3.5
Time (ps)
HEOM